



6-gingerol as an antioxidant to ameliorate kidney injury in high-fat high-fructose diet-induced metabolic syndrome in rats

Endah Wulandari¹, Salsabila Amanda Putri Andri², Vivian Soetikno^{3*} , Kusmardi⁴, Melva Louisa³, Shirly Gunawan⁵, Somasundaram Arumugam⁶

¹Master Program in Biomedical Sciences, Faculty of Medicine, Universitas Indonesia, Jakarta, Indonesia.

²Undergraduate Program in Medicine, Faculty of Medicine, Universitas Indonesia, Jakarta, Indonesia.

³Department of Pharmacology and Therapeutics, Faculty of Medicine, Universitas Indonesia, Jakarta, Indonesia.

⁴Department of Anatomical Pathology, Faculty of Medicine, Universitas Indonesia, Jakarta, Indonesia.

⁵Department of Pharmacology, Faculty of Medicine, Universitas Tarumanegara, Jakarta, Indonesia.

⁶Department of Pharmacology and Toxicology, National Institute of Pharmaceutical Education and Research (NIPER), Kolkata, India.

ARTICLE HISTORY

Received on: 07/05/2024

Accepted on: 26/09/2024

Available Online: 25/11/2024

Key words:

Oxidants, kidney diseases, diet, gingerol, insulin resistance, lipid accumulation.

ABSTRACT

The aim of this study is to investigate the impact of 6-gingerol (6-G) on oxidative stress in high-fat high-fructose (HFHF) diet-induced metabolic syndrome (MetS) in rats. Male Sprague-Dawley rats were randomly divided into five groups (n = 5). The control group received a standard diet. The MetS group received the HFHF diet for 16 weeks and, at Week 8, received a single dose of streptozotocin at 22 mg/kg body weight (b.w.). After eight weeks of HFHF diet feeding, the rats were dosed orally with 6-G (50, 100, or 200 mg/kg/day) once daily for another eight weeks. Urine samples were collected for N-acetyl-β-D-glucosaminidase (NAG) and creatinine analysis, whereas kidney tissue was obtained for histological evaluation and quantitative real-time polymerase chain reaction studies for p47phox, p67phox, NOX2, and NOX4. At the end of the study, the urine NAG/creatinine ratio was significantly decreased in the 6-G groups at all three doses. The 6-G treatment at all three doses markedly suppressed messenger RNA expression of p47phox, p67phox, NOX2, and NOX4. This was associated with a substantial decrease in tubulointerstitial inflammatory cells, fibrotic area, and lipid droplets in rats receiving the HFHF diet and 6-G treatment. 6-G could attenuate MetS-induced kidney injury via anti-oxidant activity, leading to improved kidney damage.

INTRODUCTION

Metabolic syndrome (MetS) is known to be a major and independent risk factor for impaired kidney function [1]. In Indonesia, half of chronic kidney disease patients undergoing hemodialysis suffered from MetS, and the rest were detected as having pre-MetS [2]. Furthermore, a meta-analysis showed that the risk of developing impaired kidney function in MetS was around 1.34 times higher than those without MetS [3]. Obesity and MetS-related impaired kidney function are associated with

glomerular basement membrane thickening, tubular atrophy, interstitial fibrosis, and a progressive reduction in kidney function leading to end-stage kidney disease [1,4,5].

Excessive intake of lipids, carbohydrates, and saturated fatty acids stimulates lipid accumulation in adipocytes and non-adipose tissue, such as in the kidney leading to systemic oxidative stress due to increased nicotinamide adenine dinucleotide phosphate (NADPH) oxidase (Nox) activity, chronic inflammation, tissue dysfunction, and low antioxidant defense [6–8]. Previous studies have demonstrated that in obese Zucker rats, there was an upregulation of both Nox2 and Nox1 associated with superoxide generation in the kidney vasculature [9]. The imbalance of oxidants/prooxidants plays a critical role in the occurrence of MetS. This increase in oxidative stress can contribute to the pathogenesis of MetS-induced kidney dysfunction, favoring the appearance of decreased creatinine

*Corresponding Author

Vivian Soetikno, Department of Pharmacology and Therapeutics, Faculty of Medicine, Universitas Indonesia, Jakarta, Indonesia.
E-mail: vivian.soetikno@ui.ac.id

clearance, proteinuria, and high blood urea nitrogen (BUN) levels [3–5]. Recently, Huang *et al.* [10] reported an increase in the urinary N-acetyl-β-D-glucosaminidase (NAG)/creatinine ratio in diabetic kidney disease patients and proved that this ratio is a valuable biomarker for predicting advanced diabetic kidney disease [10]. A previous study conducted by Rohman *et al.* [11] that giving a high-fat high-carbohydrate diet and streptozotocin injection to Sprague Dawley rats for 8 weeks succeeded in showing symptoms of MetS that resemble those in humans.

6-gingerol (6-G), the most abundant phenolic and bioactive compound in ginger (*Zingiber officinale* Roscoe), has been shown to have different pharmacological and physiological effects including analgesic, gastroprotective, hepatoprotective, anti-oxidant, anti-hyperglycemic, and anti-hyperlipidemic activities [12–15]. Almatroodi *et al.* [16] have demonstrated that the administration of 6-G could restore fasting blood glucose levels, hyperlipidemia, and malondialdehyde (MDA) levels and augment the antioxidant enzyme levels in the kidneys of diabetic rats. Due to its low toxicity and diverse beneficial effects, 6-G is a promising drug candidate. Therefore, the current study evaluated the impact of 6-G in ameliorating high-fat high-fructose (HFHF) diet-induced kidney dysfunction in a MetS rat model.

MATERIAL AND METHODS

Animal preparation

Eight-week-old male Sprague Dawley rats weighing 180–220 g were obtained from the National Agency of Drug and Food Control, Jakarta, Indonesia. The study protocol was approved by the Faculty of Medicine, Universitas Indonesia's Institutional Animal Care and Use Committee approved all animal procedures (KET-945/UN2.F1/ETIK/PPM.00.02/2021). The animals were housed between 25°C–30°C, had a 12-hour cycle of light and dark cycle, and were allowed free access to food and water. Before the trial, all animals were given a week to adjust to the new environment.

Experimental protocols

The animals were randomly divided into five groups, with five animals in each group (Table 1). Rats in the normal control group (I; N) received a standard pellet diet (304 kcal/100 g with 4% as fat, 20% as protein, 47% as carbohydrate, 12% as water, and 17% as mineral) while rats in the other groups (II–V) received an HFHF diet [474 kcal/100 g with 29.02% as fat, 21.31% as protein, 31.92% as carbohydrate, 12.60% as water, and 5.15% as ash along with 55% fructose by gavage (2 times daily, 1.5 ml/day)] and at Week 8, a single dose (22 mg/kg) of streptozotocin [STZ; Santa Cruz Biotechnology, USA (CAS 18883-66-4)] was intraperitoneally injected after the rats fasted for 8 hours. All diets were given throughout the study period of 16 weeks. The 16-week study period was selected based on an earlier study in mice fed an high fat diet (HFD), where oxidative stress and mitochondrial dysfunction were shown in renal cortex cell culture [17]. 6-G (Actin Chemicals™, Chengdu, China) was given to rats in groups III–V at doses of 50, 100, and 200 mg/kg/day, respectively, after confirmed MetS, namely fasting

Table 1. Experimental groups.

Group number	Group	Code name	Treatment plan
I	Normal control	N	Rats were given free access to a standard pellet diet
II	MetS control	HFHF	Rats were given HFHF diet and intraperitoneally injected with freshly prepared STZ (22 mg/kg) in 0.01 M citrate buffer pH 4.5
III	MetS + 6-G 50	6-G 50	The MetS rats were treated with 6-G at a dose of 50 mg/kg/day
IV	MetS + 6-G 100	6-G 100	The MetS rats were treated with 6-G at a dose of 100 mg/kg/day
V	MetS + 6-G 200	6-G 200	The MetS rats were treated with 6-G at a dose of 200 mg/kg/day

blood glucose levels >250 mg/dl, hypertriglyceridemia >150 mg/dl, and obesity (Lee's index > 300; Lee's index formula = $(b.w. [g]^{0.33}/naso-anal\ length [cm]) \times 10^3$) which were assessed at Week 8 after the HFHF diet and STZ injection. The 6-G dose applied in this study was derived from earlier investigations. The maximum dose used in this study was based on 1/10 of the LD50 value of gingerol [18], whereas the medium and minimum doses were calculated based on a geometric series of the maximum dose. The rats' b.w., length, and fasting blood glucose levels were assessed every week during the study. At 16 weeks following the administration of the HFHF diet or regular diet and 6-G, all rats were anesthetized with a single i.p. injection of ketamine/xylazine (87 and 13 mg/kg b.w.), and their left kidneys were excised. Half of the left kidney was immediately snap-frozen in liquid nitrogen and stored at –80°C until analysis, while the remaining excised left kidney was fixed in 10% neutral buffer formaldehyde and used for the histopathological analysis.

Estimation of biochemical parameters

Blood from the ventricle was collected and placed in a serum separator vacutainer tube. The blood was allowed to stand for 30 minutes at room temperature to separate the serum, and then the blood was centrifuged at 1,000 g, 4°C, for 10 minutes. Serum was used to measure glucose, insulin, creatinine, and urea. Fasting serum glucose was assessed using Autocheck® Glucare glucometer (Medical Technology Promedr, St. Ingbert, Germany). Rat insulin assay determinations were done by the sandwich enzyme-linked immunosorbent assay (ELISA) method using kits (E-EL-R3034) purchased from Elabscience Biotechnology Inc., Houston, TX. Homeostasis model assessment for insulin resistance (HOMA-IR) values for insulin resistance (IR) measurement was obtained through analysis of fasting serum glucose and fasting serum insulin levels at the end of the study with the following formula, $HOMA-IR = (fasting\ serum\ glucose [mg/dl] \times fasting\ serum\ insulin [\mu U/ml])/405$ [19]. Serum creatinine and urea were analyzed using the ultraviolet-visible spectrophotometric diagnostic kits obtained from Diasys, Diagnostic Systems GmbH, Germany. The 24-hour urine was also collected by placing individual rats in metabolic cages

before sacrifice. It was then used to measure protein, creatinine (Cr), and NAG levels. Urine protein and urine Cr were measured using the Bradford and Jaffe methods, respectively. NAG levels were quantified with rat rat-specific ELISA kit (CSB-E07443r, Cusabio, Houston, TX). Calculation of Cr clearance was carried out using the formula: creatinine clearance (CCr; ml/minute) = urine creatinine (mg/dl) x 24-hours urine volume (ml)/plasma creatinine (mg/dl) x 1,440 (minutes). Finally, the urinary NAG to Cr ratio was calculated as NAG/Cr to predict the progression of kidney damage due to MetS.

Measurement of kidney lipid peroxidation and glutathione peroxidase (GPx) activity

The extent of lipid oxidation in kidney tissues was evaluated using the Thiobarbituric acid (TBA) reactive substances method, in which 2-TBA reacted with MDA and resulted in a color compound. The kidney level of MDA was determined using TBA (CAS # 504-17-6) and trichloroacetic acid (TCA) (CAS # 76-03-9) assay kits (Merck, NJ). In brief, kidney tissues were rinsed, weighed as much as 50 mg added 1,800 μ l H₂O, vortexed, then added 1,000 μ l of 20% TCA solution and 2,000 μ l of 0.67% TBA solution, incubated for 10 minutes at 96°C–100°C, followed by centrifugation at 3,000 rpm for 10 minutes at 4°C, and the supernatant was determined using spectrophotometer at a wavelength of 530 nm. GPx activity was measured using an ELISA kit (MBS1600242, MyBioSource, San Diego, CA). The 96 wells were filled with a total of 40 μ l of kidney homogenate samples, followed by the addition of 10 μ l of anti-GPx antibody and 50 μ l of streptavidin-HRP, incubated at 37°C for 10 minutes, then read using a spectrophotometer at a wavelength of 450 nm.

Measurement of gene expression kidney tissue p47phox, p67phox, NOX2, and NOX4

Ribonucleic acid (RNA) was extracted from kidney tissues suspended in RNA *later* solution (ThermoFisher, USA, catalog #AM7020) by homogenization in a Quick-RNA isolation kit (Zymo Research, Freiburg, Germany). RNA concentration and purity were then measured using a Nanodrop 1,000 spectrophotometer (Thermo Scientific) at a wavelength of 260 nm. Samples with high purity ($A_{260/280} > 1.8$) were continued for complementary DNA (cDNA) isolation. cDNA synthesis was accomplished on 1 μ g of high-purity RNA using the ReverTra Ace qPCR RT Master Mix with gDNA remover (Toyobo, Osaka, Japan) according to the manufacturer's instructions. The resulting cDNA was used as a template for quantitative real-time polymerase chain reaction analysis. The primers used are listed in Table 2. Gene quantification was performed in duplicate on the LightCycler[®] 480 Instrument (Roche Applied Sciences). Data were normalized by β -actin values. All reactions were performed similarly: 95°C for 10 seconds, followed by 45 cycles of 95°C for 15 seconds and 60°C for 1 minute. The results were analyzed using the Livak ($2^{-\Delta\Delta Ct}$) method.

Assessment of lipid accumulation, tubulointerstitial inflammation, and fibrosis in kidney tissues

At the end of the study, a necropsy was done. The left kidney tissues were weighed and fixed in 10% neutral buffer

Table 2. Primer sequence.

Gene	Primer	Sequence
β -actin	Forward	5'-TCT CAA GCC TCA AGT AAC AAG C-3'
	Reverse	5'-ATG AGG TAA AGC CCG TCA GC-3'
NOX-2	Forward	5'-ACC CTC CTA TGA CTT GGA AAT G-3'
	Reverse	5'-TGA TGA CCA CCT TCT GTT GAG-3'
NOX-4	Forward	5'-AAA CAC CTC TGT CTG CTT GT-3'
	Reverse	5'-GTA TTC TGG CCC TTG GTT GTA-3'
P47phox	Forward	5'-ATG ACA GCC AGG TGA AGA AG-3'
	Reverse	5'-CGA TAG GTC TGA AGG ATG ATG G-3'
P67phox	Forward	5'-GGT GGT AGC GAT CTT CAG TTA T-3'
	Reverse	5'-CTT CCA GCC ATT CTT CAT TCA C-3'

formalin solution for 24 hours at room temperature. The tissues were subsequently dehydrated in varying concentrations of alcohol, cleared in xylene, and embedded in paraffin. Thin tissue sections (1–3 μ m thickness) were produced via slicing and subjected to staining with Hematoxylin and eosin (H&E) or Masson's trichrome (MT) stains. Fifteen photomicrographs were examined for each section by light microscopy and were recorded using 10 and 40 \times lenses. The degree of tubulointerstitial fibrosis was assessed according to a previous study [20]. Quantitative criteria for tubulointerstitial fibrosis using the following scores: 0, tubulointerstitial fibrosis in up to 5% of the cortical area; 1, mild-tubulointerstitial fibrosis in 6%–25% of the cortical area; 2, moderate-tubulointerstitial fibrosis in 26%–50% of the cortical area; 3, severe-tubulointerstitial fibrosis in >50% of the cortical area. The severity of tubulointerstitial inflammatory cell infiltration was assessed according to the following score: 0, no leukocytes in photomicrograph; 1, occasional infiltration of single leukocytes visible; 2, focal infiltration of leukocytes; 3, coalescing leukocytes; 4, diffuse infiltration of leukocytes throughout the field of view. The size of fat cells was calculated using Image-J software (Media Cybernetics, USA). The scoring system of all histopathological analyses was confirmed using two independent scorers blinded to sample identification.

Statistical analysis

Data were presented as the mean \pm SD and the groups were compared using One-Way ANOVA followed by multiple comparisons using Tukey's test. Analysis was done using SPSS software version 23.0 (USA). The level of statistical significance was defined as $p < 0.05$.

RESULTS

Effects of 6-G on b.w., HOMA-IR, and triglycerides

b.w. was the same in all groups, but at the end of the study (16 weeks), b.w. increased significantly in each group. Compared with rats in the standard diet group (N), there was a significant increase in b.w. in rats that received the HFHF diet. After continuous administration of 6-G doses of 100 and 200 mg/kg/day, b.w. decreased significantly compared with the HFHF group (Fig. 1A). HOMA-IR was assessed to evaluate IR. HOMA-IR increased significantly in the HFHF group compared

with the N group. Interestingly, after 6-G administration at all three doses, HOMA-IR decreased, and the decrease was significant at doses of 50 and 200 mg/kg/day (Fig. 1B). Serum triglyceride was also significantly increased in the HFHF diet-fed rats by 9.5-fold as compared to that of standard diet fed-rats. 6-G treatment at all three doses ameliorated the hypertriglyceridemia in a dose-dependent manner (Fig. 1C).

Effects of 6-G on proteinuria, creatinine clearance, urea serum, and urinary NAG/creatinine ratio

Next, we evaluated proteinuria, creatinine clearance, urea serum, and urinary NAG/creatinine ratio to assess MetS-related kidney injury. As shown in Fig. 1D–G, rats in the HFHF group experienced increased urinary protein excretion, BUN, and urinary NAG/Cr ratios and decreased CCr compared to rats in the standard diet group. Administration of 6-G at all three doses significantly reduced urinary protein excretion and BUN compared to the HFHF group. The urine NAG/Cr ratio can also be normalized by 6-G, especially at 50 and 200 mg/kg/day doses. Creatinine clearance could also be increased by administering 6-G at all three doses, although this was insignificant compared to the HFHF group.

Effects of 6-G on lipid peroxidation and GPx activity in kidney tissues

By evaluating the levels of MDA and GPx, the effects of 6-G on the redox state in the kidneys of the rats on the standard

diet and the HFHF diet were determined. HFHF diet-induced MetS rats showed a significant increase in MDA by 1.9-fold (Fig. 2A) and a significant decrease in GPx activity by 2.3-fold compared to the rats on the standard diet (Fig. 2B). Treatment with 6-G for eight weeks improved the altered oxidative stress levels in HFHF diet-induced MetS rats, resulting in decreased MDA levels and increased GPx activity.

Effects of 6-G on gene expressions of NOX2, NOX4, p47phox, and p67phox in kidney tissues

The HFHF diet-induced MetS rats showed noticeable oxidative stress in the kidney. The gene expression level of NOX2 was significantly increased by 6.2-fold, NOX4 by 5.8-fold, p47phox by 5.5-fold, and p67phox by 21.4-fold compared with those of the standard diet rats (Fig. 2C–F). Administration of 6-G for eight weeks at all three doses significantly reduced the expression of the NOX4 and p47phox genes, while 6-G significantly reduced the expression of the NOX2 gene only at doses of 100 and 200 mg/kg/day compared to the HFHF group. 6-G also reduced p67phox gene expression, though it was not statistically significant compared to the HFHF group.

Effects of 6-G on lipid accumulation, tubulointerstitial inflammatory cells, and tubulointerstitial fibrosis in kidney tissues

After receiving the HFHF diet for 16 weeks, the kidney tissue of the rats showed an increase in the

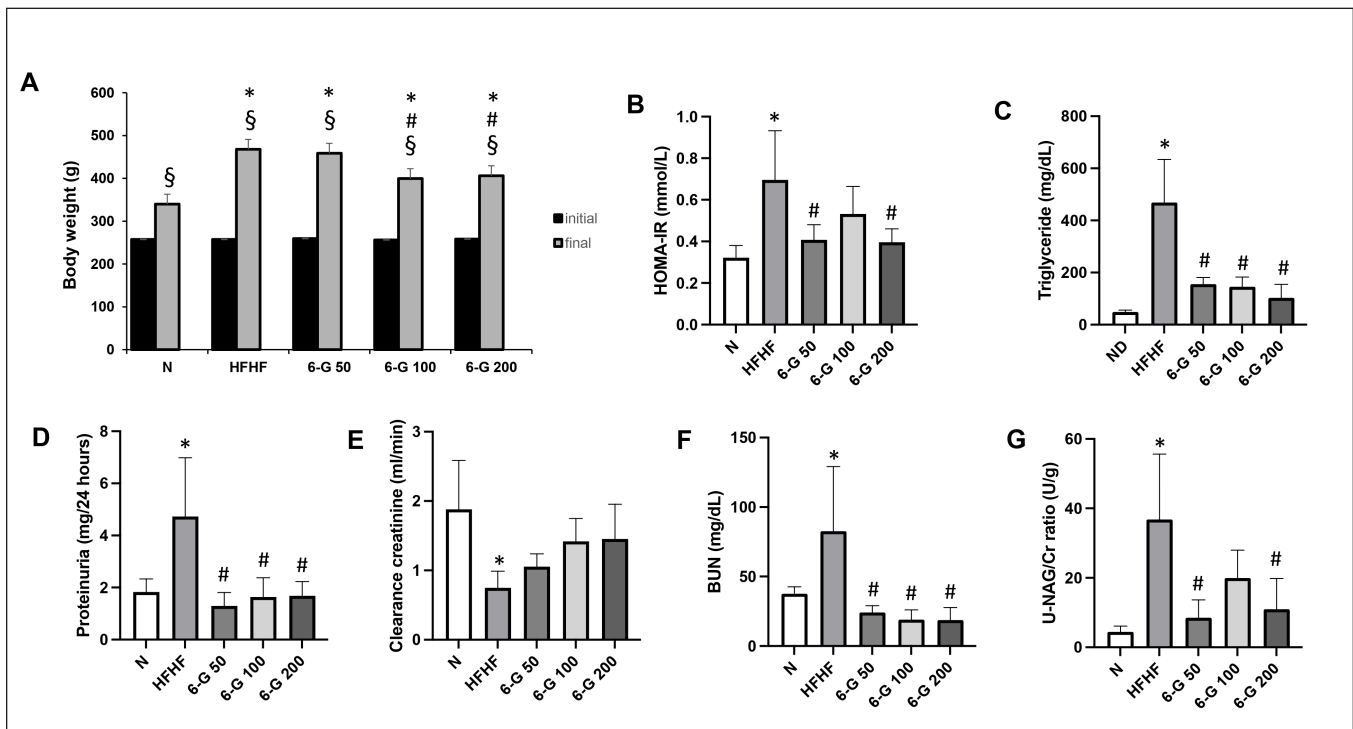


Figure 1. Effects of 6-G (50, 100, and 200 mg/kg) on HFD-induced changes in b.w., HOMA-IR, triglyceride serum, and kidney function test. (A) Changes in b.w. throughout the study period, (B) HOMA-IR values, (C) Triglyceride serum, (D) Proteinuria, (E) Creatinine clearance, (F) BUN, (G) Urinary NAG/Creatinine ratio. Rats were fed with HFD for 16 weeks; administration of 6-G started after MetS was confirmed at Week 8 and lasted till the end of the experiment. Data are expressed as means \pm SD ($n = 5$ rats per group). Mean values between groups were compared using One-way ANOVA followed by Tukey's multiple comparisons test. Mean values within groups were compared using a paired T-test. * $p < 0.05$ vs N; # $p < 0.05$ versus HFHF; § $p < 0.05$ versus initial in each group.

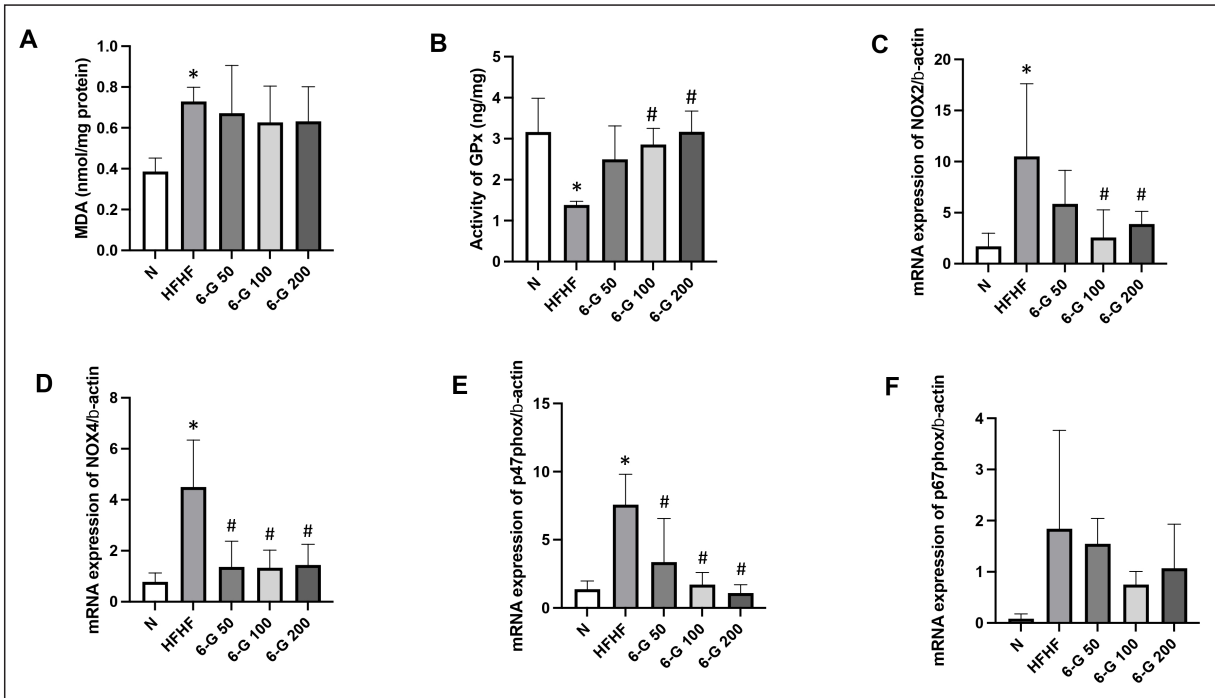


Figure 2. Effects of 6-G on kidney redox profile. 6-G showed antioxidant activity by the reduction levels of (A) MDA, (B) increased activity of GPx, (C) Effect of 6-G on the renal gene expressions of NOX2, (D) NOX4, (E) p47-phox, and (F) p67-phox. The results are expressed as means \pm SD ($n = 5$ rats per group). Statistical analysis was performed by One-way ANOVA followed by Tukey's multiple comparison test. * $p < 0.05$ versus N; # $p < 0.05$ vs HFHF.

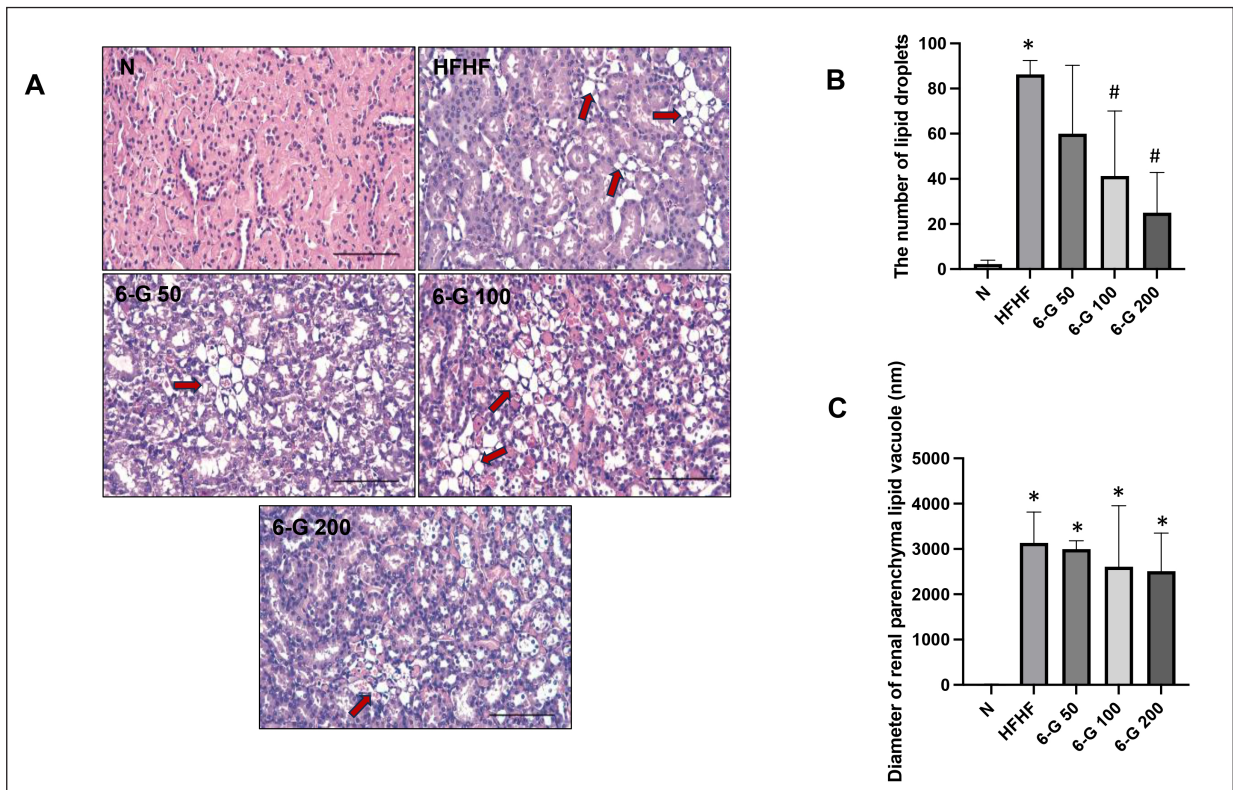


Figure 3. Effect of 6-G on kidney lipid accumulation. (A) Representative microscopic pictures of H&E-stained kidney lipid accumulation of N group, HFHF group, 6-G 50 group, 6-G 100 group, and 6-G 200 group. (B) Analysis of the number of lipid droplets in the kidney section and (C) The diameter of the lipid vacuole in the kidney section. Images were captured at 400x magnification. Scale bar, 50 μ m. Red arrows: lipid vacuole. Data are expressed as means \pm SD ($n = 5$ rats per group). Mean values of the number of lipid droplets and lipid vacuole size were compared using One-way ANOVA followed by Tukey's multiple comparisons test. * $p < 0.05$ vs N; # $p < 0.05$ versus HFHF.

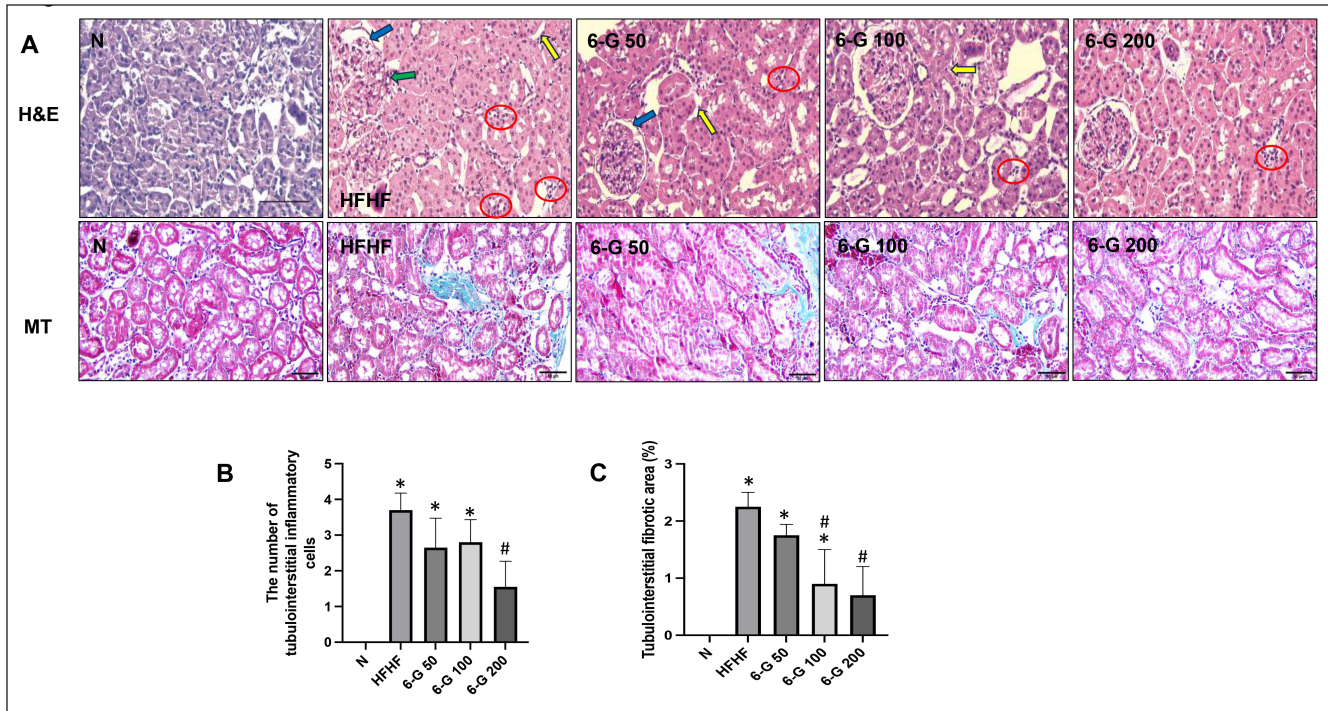


Figure 4. Effect of 6-G on histopathological changes in kidney tissues using H&E stain. (A) Representative microscopic pictures of H&E-stained kidney sections of N group, HFHF group, 6-G 50 group, 6-G 100 group, and 6-G 200 group. (B) Representative microscopic pictures of MT staining of renal fibrosis of N group, HFHF group, 6-G 50 group, 6-G 100 group, and 6-G 200 group; The blue area indicates fibrosis. (C) Analysis of the number of tubulointerstitial inflammatory cells, and (D) Analysis of tubulointerstitial fibrotic area. Images were captured at 400x magnification. Scale bar, 50 μ m. Red circles: infiltration of polymorphonuclear cells. Blue arrows: thickening of the glomerular basement membrane. Green arrows: arteriolopathy. Yellow arrows: tubular atrophy. Data are expressed as means \pm SD ($n = 5$ rats per group). Mean values of the number of tubulointerstitial inflammatory cells and tubulointerstitial fibrotic area were compared using One-way ANOVA followed by Tukey's multiple comparisons test. * $p < 0.05$ vs N; # $p < 0.05$ versus HFHF.

accumulation of lipid droplets in the renal parenchymal tissue (Fig. 3A; HFHF). This was also confirmed by the rise in the number of lipid droplets (Fig. 3B) as well as in the diameter of lipid vacuole (Fig. 3C). In addition, as it was demonstrated in Figure 4, the kidney section of the standard diet-fed rats was healthy with no lesion, and the glomerulus and tubules could be seen in intact forms (Fig. 4A; N). On the contrary, there was an increase in inflammatory cells in the tubulointerstitial area in HFHF diet-fed rats (Fig. 4A; HFHF and Fig. 4B). Histological examination of kidney tissue in the HFHF diet-fed rats that received 6-G showed improvements by reducing the number of inflammatory cells in the tubulointerstitial area and reducing the accumulation of lipid droplets in the renal parenchymal tissue. These improvements seemed to be more pronounced in the 6-G 200 mg/kg/day dose-receiving group (Figs. 3 and 4). Furthermore, MT staining demonstrated increased tubulointerstitial fibrosis in the HFHF diet-fed rats compared with the standard diet-fed rats, and 6-G treatment at all three doses greatly reduced the fibrosis in HFHF-induced MetS kidney tissue (Fig. 4A; MT and C).

DISCUSSION

In this study, we have shown that 6-G, a bioactive metabolite of ginger, had beneficial effects in ameliorating kidney injury in HFHF diet-induced MetS rats by modulating oxidative stress. Our findings showed that 16-week HFHF

feeding induced obesity and IR in rats. These HFHF diet-fed rats exhibited abnormal accumulation of lipids in the kidney. The lipid accumulation in the kidney that we found in this study represented the increased oxidative stress and accompanying inflammatory processes that lead to kidney injury. The manifestations of kidney injury in HFD diet-fed rats include tubular hypertrophy, increased tubulointerstitial inflammatory cell infiltration, tubular fibrosis, and glomerular basement membrane thickening, and the pathological outcome was proteinuria, reduced CCR, increased BUN and urinary ratio of NAG/Cr. 6-G treatment ameliorated kidney injury by significantly lowering proteinuria, urinary NAG/Cr ratio, urea serum, and increasing CCr. Furthermore, 6-G improved insulin sensitivity and maintained the b.w. of MetS animals throughout the study period.

In this study, we employed high-fat, high-fructose, and low-dose STZ to induce MetS in rats. The ensuing MetS components were IR, obesity, and hyperlipidemia. Similarly, previous studies have also proven that giving an HFHF diet and STZ injection can induce MetS in rats, which was characterized by increased triglyceride, total cholesterol, LDL-cholesterol, and fasting plasma glucose levels and decreased HDL-cholesterol levels [15,21]. Furthermore, HFD-induced ectopic lipid accumulation in non-adipose tissue, such as in the kidney, liver, pancreas, skeletal muscle, and heart, is closely related to IR [22–25]. Likewise, we showed that feeding an HFHF diet

for 16 weeks led to lipid accumulation in kidney tissue and IR. Interestingly, 6-G administration attenuated HFHF diet-induced b.w. and kidney lipid accumulation and suppressed HFD-induced IR.

Kidney lipid accumulation and lipotoxicity might drive oxidative stress, inflammation, and fibrosis, leading to kidney dysfunction [26,27]. Numerous studies have established that HFD-induced lipid accumulation can result in changes to renal structure and function, including a reduction in glomerular filtration rate and an increase in urine microalbuminuria, at least in part due to a prooxidant/antioxidant imbalance [28–30]. Martínez-García *et al.* [31] have demonstrated that kidney lipid accumulation and IR were associated with inflammation, oxidative stress, and endoplasmic reticulum stress in podocyte cell lines-treated palmitic acid. In the present study, we also found that HFHF diet-fed rats for 16 weeks caused kidney lipid accumulation, as indicated by an increase in the number and area of lipid droplets in the renal parenchyma. Treatment with 6-G at all three doses reduced kidney lipid accumulation, including the number and size of kidney lipid vacuoles.

Moreover, 6-G treatment significantly reduced renal dysfunction biomarkers such as proteinuria, BUN, and urinary NAG/Cr ratio and increased CCr compared to HFD diet-fed rats. These results showed that 6-G protects renal function in HFD diet-induced kidney dysfunction in MetS rats, at least partially due to reduced kidney parenchymal lipid accumulation. Previous reports also supported that 6-G significantly improved MetS-induced renal dysfunction [16,32].

Diets, particularly high in fat or carbohydrates, are associated with oxidative stress by increasing the amounts of lipid peroxidation products and protein carbonylation while decreasing the antioxidant defence status [33]. Proteins, lipids, and nucleic acids undergo structural and functional damage due to oxidative stress. MDA, 4-hydroxynonenal, and isoprostane can be produced by the oxidation of lipids, mainly unsaturated fatty acids [34]. Antioxidant enzymes, including GPx, are essential in maintaining reactive oxygen species (ROS) homeostasis and protecting cells from oxidative damage [35]. In the present study, we showed that HFHF caused oxidative stress, evidenced by changes in the levels of MDA and GPx in the kidney tissues. 6-G treatment attenuated HFHF-diet-induced oxidative stress by enhancing the kidney GPx activity and decreasing the kidney MDA levels.

The origin of ROS is very diverse, and one of the enzymes in the body that can increase ROS production is NADPH oxidase (Nox) [36]. The Nox complex consists of two membrane subunits, Nox2 and p22-phox, and several cytosolic subunits, namely p47-phox, p67-phox, and p40-phox; when activated, the cytosolic subunit will translocate to the membrane subunit and produce ROS [37]. Nox4 is the primary source of ROS in the kidney, and studies have shown that the expression was increased in a high glucose and obesity state, which induces renal hypertrophy [9]. The HFHF diet-induced MetS animals reported here showed significantly increased Nox2, p47-phox, p67-phox, and Nox4 after 16 weeks of the study compared to the standard-diet animals. These findings align with earlier studies that showed

increased Nox expression in response to high glucose levels and excessive ROS generation [38].

Long-term HFD feeding has been shown to cause not only ectopic lipid accumulation in the kidney but also activation of pro-fibrotic pathways in that organ [16]. In addition, several studies have also demonstrated that HFD could induce renal proximal tubular injury [39,40]. Previous studies have demonstrated that the damaging effect of MetS on rat kidneys was caused by increased renin-angiotensin-aldosterone system (RAAS) and ROS activity in the kidneys, which is accompanied by a decrease in angiotensin converting enzyme-2, glutathione, and superoxide dismutase, and an increase in NADPH enzyme activities in the kidneys [41,42]. In accordance with previous studies, we also found that HFHF feeding for 16 weeks caused damage to the kidney proximal tubule, glomeruli, and fibrosis in the kidney tissues compared to the standard diet-fed rats. Administration of 6-G in all three doses for eight weeks could attenuate HFHF-induced damage in the kidney tubules and glomeruli and reduce kidney fibrosis, at least in part due to decreased oxidative stress. A previous report has also indicated that 6-G prevents tubular and glomerular disruption in kidney tissue [43]. Rodrigues *et al.* [32] have also reported that gingerol attenuated septic acute kidney injury, at least in part due to decreased oxidative stress and inflammatory response.

The main advantage of the present study is that we were able to prove that administration of 6-G for 8 weeks in MetS rats reduced fibrosis, and lipid accumulation in the kidneys as well as improved kidney function, especially at a dose of 200 mg/kg/day through reducing oxidative stress. However, the present study also has some limitations that need to be acknowledged, namely (1) Urinary NAG/Cr ratio was measured once, while repeated testing during the study could better show the effectiveness of 6-G in improving kidney function, and (2) to further ensure that there is dose-dependency of 6-G, further study is needed, including extending the duration of 6-G administration.

Future research also could, for instance, investigate how 6-G mechanisms ameliorate lipid accumulation in non-adipose tissue through reducing inflammation processes and endoplasmic reticulum stress as well as the RAAS pathway. Such research could contribute to identifying specific strategies for the successful management of MetS in humans.

In conclusion, we showed the beneficial effects of 6-G against HFHF-induced kidney injury through its antioxidant activity. It is also conceivable that the urinary NAG/creatinine ratio could be used as a biomarker in MetS-induced kidney injury.

ACKNOWLEDGMENTS

This work was supported by Universitas Indonesia [Grant number: NKB-1261/UN2.RST/HKP.05.00/2022].

ETHICAL APPROVALS

The study protocol was approved by the Institutional Animal Care and Use Committee of Faculty of Medicine, University of Indonesia, Indonesia (Approval No. KET-945/UN2.F1/ETIK/PPM.00.02/2021).

CONFLICTS OF INTEREST

The authors report no financial or any other conflicts of interest in this work.

AUTHOR CONTRIBUTIONS

All authors made substantial contributions to conception and design, acquisition of data, or analysis and interpretation of data; took part in drafting the article or revising it critically for important intellectual content; agreed to submit to the current journal; gave final approval of the version to be published; and agree to be accountable for all aspects of the work. All the authors are eligible to be an author as per the international committee of medical journal editors (ICMJE). requirements/guidelines.

DATA AVAILABILITY

All the data is available with the authors and shall be provided upon request.

PUBLISHER'S NOTE

This journal remains neutral with regard to jurisdictional claims in published institutional affiliation.

USE OF ARTIFICIAL INTELLIGENCE (AI)-ASSISTED TECHNOLOGY

The authors declares that they have not used artificial intelligence (AI)-tools for writing and editing of the manuscript, and no images were manipulated using AI.

REFERENCES

- Ciardullo S, Ballabeni C, Trevisan R, Perseghin G. Metabolic syndrome, and not obesity, is associated with chronic kidney disease. *Am J Nephrol.* 2021;52:666–72. doi: 10.1159/000518111
- Syukri M, Virnardo R, Salwani D, Abdullah Sofyan H, Marthoenis. The prevalence and associated factors of metabolic syndrome among patients with end-stage renal failure undergoing hemodialysis in Indonesia. *Diabetes Metab Syndr.* 2020;14:2069–72. doi: 10.1016/j.dsx.2020.10.019
- Wu N, Qin Y, Chen S, Yu C, Xu Y, Zhao J, *et al.* Association between metabolic syndrome and incident chronic kidney disease among Chinese: a nation-wide cohort study and updated meta-analysis. *Diabetes Metab Res Rev.* 2021;37:e3437. doi: 10.1002/dmrr.3437
- Pammer LM, Lamina C, Schultheiss UT, Kotsis F, Kollerits B, Stockmann H, *et al.* GCKD investigators. association of the metabolic syndrome with mortality and major adverse cardiac events: a large chronic kidney disease cohort. *J Intern Med.* 2021;290:1219–32. doi: 10.1111/joim.13355
- DeBoer MD, Filipp SL, Musani SK, Sims M, Okusa MD, Gurka M. Metabolic syndrome severity and risk of CKD and worsened GFR: the Jackson Heart Study. *Kidney Blood Press Res.* 2018;2:555–67. doi: 10.1159/000488829
- Nono Nankam PA, Ngudefack TB, Goedecke JH, Blüher M. Contribution of adipose tissue oxidative stress to obesity-associated diabetes risk and ethnic differences: focus on women of African ancestry. *Antioxidants* 2021;10:622. doi: 10.3390/antiox10040622
- Fernández-Sánchez A, Madrigal-Santillán E, Bautista M, Esquivel-Soto J, Morales-González A, Esquivel-Chirino C, *et al.* Inflammation, oxidative stress, and obesity. *Int J Mol Sci.* 2011;12:3117–32. doi: 10.3390/ijms12053117
- Huang CJ, McAllister MJ, Slusher AL, Webb HE, Mock JT, Acevedo EO. Obesity-related oxidative stress: the impact of physical activity and diet manipulation. *Sports Med Open.* 2015;1:32. doi: 10.1186/s40798-015-0031-y
- Muñoz M, López-Oliva ME, Rodríguez C, Martínez MP, Sáenz-Medina J, Sánchez A, *et al.* Differential contribution of Nox1, Nox2 and Nox4 to kidney vascular oxidative stress and endothelial dysfunction in obesity. *Redox Biol.* 2020;28:101330. doi: 10.1016/j.redox.2019.101330
- Huang Q, Fei X, Zhan H, Gong J, Zhou J, Zhang Y, *et al.* Urinary N-acetyl-β-d-glucosaminidase-creatinine ratio is a valuable predictor for advanced diabetic kidney disease. *J Clin Lab Anal.* 2023;37:e24769. doi: 10.1002/jcla.24769
- Rohman MS, Lukitasari M, Nugroho DA, Widodo N, Nugrahini NIP, Sardjono TWM. Development of an Experimental model of metabolic syndrome in sprague dawley rat. *Res J Life Sci.* 2017;4:76–86.
- Anh NH, Kim SJ, Long NP, Min JE, Yoon YC, Lee EG, *et al.* Ginger on human health: a comprehensive systematic review of 109 randomized controlled trials. *Nutrients.* 2020;12:157. doi: 10.3390/nu12010157
- Nikkhah Bodagh M, Maleki I, Hekmatdoost A. Ginger in gastrointestinal disorders: a systematic review of clinical trials. *Food Sci Nutr.* 2018;7:96–108. doi: 10.1002/fsn3.807
- Unuofin JO, Masuku NP, Paimo OK, Lebelo SL. Ginger from Farmyard to Town: nutritional and pharmacological applications. *Front Pharmacol.* 2021;12:779352. doi: 10.3389/fphar.2021.779352
- Gunawan S, Munika E, Wulandari ET, Ferdinal F, Purwaningsih EH, Wuyung PE, *et al.* 6-gingerol ameliorates weight gain and insulin resistance in metabolic syndrome rats by regulating adipocytokines. *Saudi Pharm J.* 2023;31:351–8. doi: 10.1016/j.jsps.2023.01.003
- Almatroodi SA, Alnuqaydan AM, Babiker AY, Almogbel MA, Khan AA, Husain Rahmani A. 6-Gingerol, a bioactive compound of ginger attenuates renal damage in streptozotocin-induced diabetic rats by regulating the oxidative stress and inflammation. *Pharmaceutics.* 2021;13:317. doi: 10.3390/pharmaceutics13030317
- Sun Y, Ge X, Li X, He J, Wei X, Du J, *et al.* High-fat diet promotes renal injury by inducing oxidative stress and mitochondrial dysfunction. *Cell Death Dis.* 2020;11:914. doi: 10.1038/s41419-020-03122-4
- Benny M, Shylaja MR, Antony B, Gupta NK, Mary R, Anto A, *et al.* Acute and sub-acute toxicity studies with ginger extract in rats. *IJPSR.* 2021;33:2799–809. doi: 10.13040/ijpsr.0975-8232.12(5).2799-09
- Wallace TM, Levy JC, Matthews DR. Use and abuse of HOMA modeling. *Diabetes Care.* 2004;27:1487–95. doi: 10.2337/diacare.27.6.1487
- Racusen LC, Solez K, Colvin RB, Bonsib SM, Castro MC, Cavallo T, *et al.* The Banff 97 working classification of renal allograft pathology. *Kidney Int.* 1999;55:713–23. doi: 10.1046/j.1523-1755.1999.00299.x
- Hidayati L, Widodo ADW, Hidayat B. Animal models with metabolic syndrome markers induced by high fat diet and fructose. *Med Lab Technol J* 2020;6:13–20.
- Samuel VT, Shulman GI. Mechanisms for insulin resistance: common threads and missing links. *Cell.* 2012;148:852–71. doi: 10.1016/j.cell.2012.02.017
- Snel M, Jonker JT, Schoones J, Lamb H, de Roos A, Pijl H, *et al.* Ectopic fat and insulin resistance: pathophysiology and effect of diet and lifestyle interventions. *Int J Endocrinol.* 2012;2012:983814. doi: 10.1155/2012/983814
- Kume S, Uzu T, Araki S, Sugimoto T, Ishiki K, Chin-Kanasaki M, *et al.* Role of altered renal lipid metabolism in the development of renal injury induced by a high-fat diet. *J Am Soc Nephrol.* 2007;18:2715–23. doi: 10.1681/ASN.2007010089
- Li Z, Woollard JR, Wang S, Korsmo MJ, Ebrahimi B, Grande JP, *et al.* Increased glomerular filtration rate in early metabolic syndrome is associated with renal adiposity and microvascular proliferation. *Am J Physiol Renal Physiol.* 2011;301:F1078–87. doi: 10.1152/ajprenal.00333.2011

26. Mitrofanova A, Merscher S, Fornoni A. Kidney lipid dysmetabolism and lipid droplet accumulation in chronic kidney disease. *Nat Rev Nephrol.* 2023;19:629–45. doi: 10.1038/s41581-023-00741-w
27. Gyurászová M, Gurecká R, Bábíčková J, Tóthová E. Oxidative stress in the pathophysiology of kidney disease: implications for noninvasive monitoring and identification of biomarkers. *Oxid Med Cell Longev.* 2020;2020:5478708. doi: 10.1155/2020/5478708
28. Thomas G, Sehgal AR, Kashyap SR, Srinivas TR, Kirwan JP, Navaneethan SD. Metabolic syndrome and kidney disease: a systematic review and meta-analysis. *Clin J Am Soc Nephrol.* 2011;10: 2364–73. doi: 10.2215/CJN.02180311
29. Kawamoto R, Akase T, Ninomiya D, Kumagi T, Kikuchi A. Metabolic syndrome is a predictor of decreased renal function among community-dwelling middle-aged and Elderly Japanese. *Int Urol Nephrol.* 2019;12:2285–94. doi: 10.1007/s11255-019-02320-0
30. Serra-Majem L, Román-Viñas B, Sanchez-Villegas A, Guasch-Ferré M, Corella D, La Vecchia C. Benefits of the Mediterranean diet: epidemiological and molecular aspects. *Mole Asp Med.* 2019;67:1–55. doi: 10.1016/j.mam.2019.06.001
31. Martínez-García C, Izquierdo-Lahuerta A, Vivas Y, Velasco I, Yeo TK, Chen S, Medina-Gomez G. Renal lipotoxicity-associated inflammation and insulin resistance affects actin cytoskeleton organization in podocytes. *PLoS One* 2015;10:e0142291. doi: 10.1371/journal.pone.0142291
32. Rodrigues FAP, Santos ADDC, de Medeiros PHQS, Prata MMG, Santos TCS, da Silva JA, *et al.* Gingerol suppresses sepsis-induced acute kidney injury by modulating methylsulfonylmethane and dimethylamine production. *Sci Rep.* 2018;8:12154. doi: 10.1038/s41598-018-30522-6
33. Babel RA, Dandekar MP. A review on cellular and molecular mechanisms linked to the development of diabetes complications. *Curr Diabetes Rev.* 2021;17:457–73. doi: 10.2174/1573399816666201103143818
34. Grootveld M, Percival BC, Leenders J, Wilson PB. Potential adverse public health effects afforded by the ingestion of dietary lipid oxidation product toxins: significance of fried food sources. *Nutrients* 2020;12:974.
35. Zhang J, Hao H, Wu X, Wang Q, Chen M, Feng Z, *et al.* The functions of glutathione peroxidase in ROS homeostasis and fruiting body development in *Hypsizygus marmoreus*. *Appl Microbiol Biotechnol.* 2020;104:10555–70. doi: 10.1007/s00253-020-10981-6
36. Brieger K, Schiavone S, Miller FJ Jr, Krause KH. Reactive oxygen species: from health to disease. *Swiss Med Wkly.* 2012;142:w13659. doi: 10.4414/smw.2012.13659
37. Rastogi R, Geng X, Li F, Ding Y. NOX activation by subunit interaction and underlying mechanisms in disease. *Front Cell Neurosci.* 2017;10:301. doi: 10.3389/fncel.2016.00301
38. Soetikno V, Watanabe K, Sari FR, Harima M, Thandavarayan RA, Veeraveedu PT, *et al.* Curcumin attenuates diabetic nephropathy by inhibiting PKC- α and PKC- β 1 activity in streptozotocin-induced type I diabetic rats. *Mol Nutr Food Res.* 2011;55:1655–65. doi: 10.1002/mnfr.201100080
39. Xu S, Luo W, Xu X, Qian Y, Xu Z, Yu W, *et al.* MD2 blockade prevents oxLDL-induced renal epithelial cell injury and protects against high-fat-diet-induced kidney dysfunction. *J Nutr Biochem.* 2019;70:47–55. doi: 10.1016/j.jnutbio.2019.04.003
40. Yamamoto T, Takabatake Y, Takahashi A, Kimura T, Namba T, Matsuda J, *et al.* High-fat diet-induced lysosomal dysfunction and impaired autophagic flux contribute to lipotoxicity in the kidney. *J Am Soc Nephrol.* 2017;28:1534–51. doi: 10.1681/ASN.2016070731
41. El-Domiati HF, Sweed E, Kora MA, Zaki NG, Khodir SA. Activation of angiotensin-converting enzyme 2 ameliorates metabolic syndrome-induced renal damage in rats by renal TLR4 and nuclear transcription factor κ B downregulation. *Front Med (Lausanne).* 2022;9:904756. doi: 10.3389/fmed.2022.904756
42. Rodríguez-Fierros FL, Guarner-Lans V, Soto ME, Manzano-Pech L, Díaz-Díaz E, Soria-Castro E, *et al.* Modulation of renal function in a metabolic syndrome rat model by antioxidants in *Hibiscus sabdariffa* L. *Molecules.* 2021;26:2074. doi: 10.3390/molecules26072074
43. Hegazy AM, Mosaed MM, Elshafey SH, Bayomy NA. 6-gingerol ameliorates gentamicin induced renal cortex oxidative stress and apoptosis in adult male albino rats. *Tissue Cell.* 2016;48:208–16. doi: 10.1016/j.tice.2016.03.006

How to cite this article:

Wulandari E, Andri SAP, Soetikno V, Kusmardi, Louisa M, Gunawan S, Arumugam S. 6-gingerol as an antioxidant to ameliorate kidney injury in high-fat high-fructose diet-induced metabolic syndrome in rats. *J Appl Pharm Sci.* 2025;15(01):072–080.